



IUScholarWorks at Indiana University South Bend

Phase Relations of Fe-Si Alloy in Earth's Core

Lin, J.- F., Scott, H. P., Fischer, R. A., Chang, Y.- Y., Kantor, I., and Prakapenka

To cite this article:

Lin, J.- F., Scott, H. P., Fischer, R. A., Chang, Y.- Y., Kantor, I., and Prakapenka, V. B. (2009), Phase relations of Fe-Si alloy in Earth's core, *Geophys. Res. Lett.*, 36, L06306, doi:10.1029/2008GL036990.

This document has been made available through IUScholarWorks repository, a service of the Indiana University Libraries. Copyrights on documents in IUScholarWorks are held by their respective rights holder(s). Contact iusw@indiana.edu for more information.

Phase relations of Fe-Si alloy in Earth's core

Jung-Fu Lin,¹ Henry P. Scott,² Rebecca A. Fischer,³ Yun-Yuan Chang,³ Innokenty Kantor,⁴ and Vitali B. Prakapenka⁴

Received 11 December 2008; revised 27 February 2009; accepted 3 March 2009; published 28 March 2009.

[1] Phase relations of an $\text{Fe}_{0.85}\text{Si}_{0.15}$ alloy were investigated up to 240 GPa and 3000 K using *in situ* X-ray diffraction in a laser-heated diamond anvil cell. An alloy of this composition as starting material is found to result in a stabilized mixture of Si-rich *bcc* and Si-poor *hcp* Fe-Si phases up to at least 150 GPa and 3000 K, whereas only *hcp*- $\text{Fe}_{0.85}\text{Si}_{0.15}$ is found to be stable between approximately 170 GPa and 240 GPa at high temperatures. Our extended results indicate that $\text{Fe}_{0.85}\text{Si}_{0.15}$ alloy is likely to have the *hcp* structure in the inner core, instead of the previously proposed mixture of *hcp* and *bcc* phases. Due to the volumetric dominance of the *hcp* phase in the *hcp* + *bcc* coexistence region close to the outer-core conditions, the dense closest-packed Fe-Si liquid is more relevant to understanding the properties of the outer core. **Citation:** Lin, J.-F., H. P. Scott, R. A. Fischer, Y.-Y. Chang, I. Kantor, and V. B. Prakapenka (2009), Phase relations of Fe-Si alloy in Earth's core, *Geophys. Res. Lett.*, *36*, L06306, doi:10.1029/2008GL036990.

1. Introduction

[2] Geophysical and cosmochemical evidence indicates that iron is the most abundant component in the Earth's core [Birch, 1952]. However, there is a density deficit between seismic observations of Earth's core and high pressure-temperature iron, implying the presence of a certain amount of element(s) lighter than iron at an abundance of 6–10 wt% for the outer core and 2–5 wt% for the inner core [e.g., Poirier, 1994; Li and Fei, 2003]. Silicon has been proposed to be a major alloying light element in the Earth's core [e.g., Poirier, 1994; Li and Fei, 2003] based on its cosmochemical abundance, solubility in liquid Fe at high pressures and temperatures [e.g., Takafuji *et al.*, 2005; Sakai *et al.*, 2006], and thermoelastic properties in Fe-Si alloys [e.g., Lin *et al.*, 2003a, 2003b; Hirao *et al.*, 2004]. These recent results indicate that an outer core containing about 8–10 wt% Si and inner core containing about 4 wt% Si in Fe would satisfy seismological constraints, although other light elements such as oxygen and sulfur could also exist in the core [e.g., Takafuji *et al.*, 2005; Sakai *et al.*, 2006]. Studying the phase relations and thermoelastic properties of the Fe-rich Fe-Si alloy is thus essential for our understanding of Earth's core.

¹Department of Geological Sciences, Jackson School of Geosciences, University of Texas at Austin, Austin, Texas, USA.

²Department of Physics and Astronomy, Indiana University, South Bend, Indiana, USA.

³Department of Earth and Planetary Sciences, Northwestern University, Evanston, Illinois, USA.

⁴Consortium for Advanced Radiation Sources, University of Chicago, Chicago, Illinois, USA.

[3] Pure Fe is found to be stable in the hexagonal closest-packed (*hcp*) structure over a wide range of pressures and temperatures approaching suspected Earth's core conditions, whereas reports on the occurrence of a doubled *hcp*-Fe and an orthorhombic Fe at high pressures and temperatures are now mostly believed to be a result of experimental problems [e.g., Shen *et al.*, 1998; Ma *et al.*, 2004; Kuwayama *et al.*, 2008]. Theoretical calculations further suggest that the *hcp*-Fe transforms into a body-centered cubic (*bcc*) Fe at conditions close to its melting line at core pressures [e.g., Vocadlo *et al.*, 2003; Belonoshko *et al.*, 2008], but this has not been confirmed experimentally.

[4] Under ambient conditions, Fe-rich Fe-Si alloys with a Si content relevant to Earth's core (<10 wt%) are stable in the *bcc* structure. Theoretical studies have shown that addition of a few weight percent of Si into Fe can stabilize the *bcc* Fe-Si alloy at the pressure-temperature conditions of the core [Cote *et al.*, 2008a, 2008b; Vocadlo *et al.*, 2003]. Whereas earlier high pressure-temperature experiments have shown that Si alloyed with Fe can stabilize the *bcc* phase up to at least 84 GPa (compared to ~10 GPa for pure Fe) and 2400 K [Lin *et al.*, 2002a; Lin, 2002], recent studies, however, have suggested that Fe-rich Fe-Si alloys dissociate into almost pure Fe and a *b2*-structured FeSi compound [Dubrovinsky *et al.*, 2003], or a mixture of face-centered cubic (*fcc*) and *hcp* phases [Asanuma *et al.*, 2008]. Since these phases may differ in physical properties such as sound velocities, knowing the stable crystal structure of the Fe-Si alloy under relevant conditions is thus essential for our understanding of Earth's core. To decipher the phase relations of the Fe-Si alloy at extended pressure-temperature conditions relevant to Earth's core, here we have studied the phase relations of an $\text{Fe}_{0.85}\text{Si}_{0.15}$ alloy (containing 8 wt% Si) up to 240 GPa and 3000 K using *in situ* X-ray diffraction in a laser-heated diamond anvil cell (DAC).

2. Experiments

[5] The starting $\text{Fe}_{0.85}\text{Si}_{0.15}$ alloy was obtained from Goodfellow Corporation. X-ray diffraction and electron microprobe analyses showed that the sample was in the *bcc* structure and chemically homogenous. Samples measuring approximately 5–15 μm thick and 25 μm in diameter were loaded into symmetric DACs with 75–300 μm beveled diamonds or 60–180–300 μm double-beveled diamonds using Re gaskets. We also used cubic boron nitride (BN) gasket inserts in some of the experiments to prepare samples with sufficient thickness for laser heating and diffraction measurements and to avoid diffraction peaks from Re gaskets. Samples were sandwiched between dried NaCl layers in the DACs, and the NaCl was used as the thermal insulator, pressure medium, and pressure calibrant. Pressures were determined from the lattice parameter and equation of state

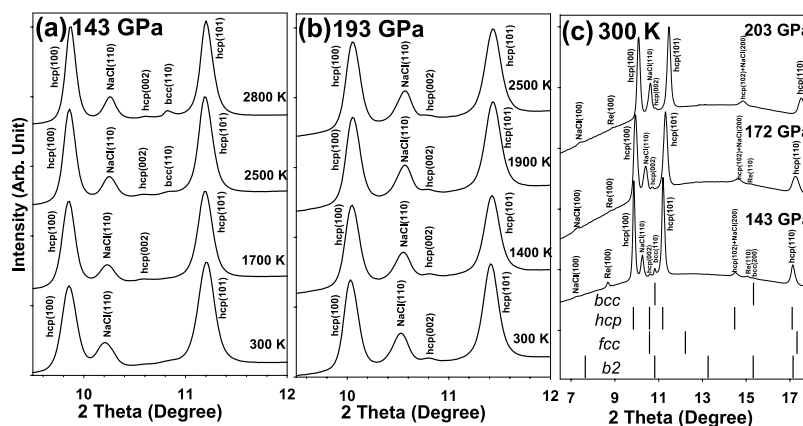


Figure 1. Representative X-ray diffraction patterns of $\text{Fe}_{0.85}\text{Si}_{0.15}$ at high pressures and temperatures. (a) Detailed spectra at 143 GPa, (b) detailed spectra at 193 GPa, and (c) full diffraction spectra after quenching from highest temperatures at high pressures (see Figure 2 for the highest temperatures). Vertical ticks in Figure 1c represent modeled diffraction peaks of *bcc*, *hcp*, *fcc*, and *b2* phases. *NaCl*, sodium chloride in the *CsCl* structure; *Re*, rhenium gasket. Note that the *b2* and *fcc* peaks were not observed in these spectra. The wavelength of the monochromatic X-ray source was 0.3344 Å.

of NaCl before heating [Fei *et al.*, 2007], and were also measured after heating. *In situ* high pressure-temperature X-ray diffraction experiments were conducted at the GeoSoilEnviroCARS sector of the Advanced Photon Source (APS), Argonne National Laboratory (ANL) [Prakapenka *et al.*, 2008]. We used two diode-pumped ytterbium infrared fiber lasers operating in single-mode continuous wave, with a wavelength of 1064 nm, and focused flat-top shapes approximately 15 μm in diameter at the sample position to laser-heat the sample from both sides of the DAC. A monochromatic beam 0.3344 Å in wavelength and 5 μm in diameter (at Full Width at Half Maximum (FWHM)) was used as the incident X-ray source and was well aligned with the laser-heating spots using the X-ray fluorescence of the sample, and the diffracted X-rays were collected by a CCD (MAR165). Graybody temperatures were determined by fitting the thermal radiation spectra between 670 and 830 nm to the Planck radiation function. The temperature uncertainty (1σ), averaged from multiple temperature measurements, ranges from 100 K to 250 K in most of the experiments.

3. Experimental Results

[6] The phase relations of the $\text{Fe}_{0.85}\text{Si}_{0.15}$ alloy have been investigated up to 240 GPa and 3000 K (Figures 1 and 2). Prior to laser heating, we compressed the *bcc*- $\text{Fe}_{0.85}\text{Si}_{0.15}$ starting material to pressures between 100 and 240 GPa at room temperature and found that all transformed to the *hcp* structure. Each sample was then laser heated, and diffraction patterns were collected at a series of temperature steps up to maximum heating temperatures as high as 3000 K (see auxiliary material for details); these data were used to constrain the phase relations as indicated in Figure 2.¹ Upon heating, the *hcp*- $\text{Fe}_{0.85}\text{Si}_{0.15}$ transitioned to a mixture of the Si-poor *hcp* and Si-rich *bcc* phases at pressures up to at least 150 GPa (Figure 2), whereas the *hcp*- $\text{Fe}_{0.85}\text{Si}_{0.15}$ phase is observed to be stable between approximately 170 GPa and 240 GPa at high temperatures. Following previous experi-

ments on the identification of the Fe-Si polymorphs [Lin *et al.*, 2002a; Lin, 2002], the occurrence of the *bcc* phase can be identified by the *bcc* (110) peak in between the *hcp* (002) and (101) peaks at high temperatures, although the intensity of the *bcc* (110) peak is relatively weaker compared with

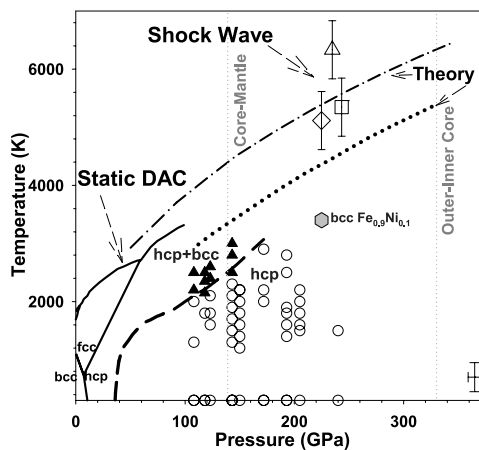


Figure 2. Observed phases from an $\text{Fe}_{0.85}\text{Si}_{0.15}$ starting material superimposed on a phase diagram of pure Fe (solid lines). The phase diagram for Fe is modified from Nguyen and Holmes [2004] and includes data from static DAC experiments [Shen *et al.*, 1998; Ma *et al.*, 2004]. Typical error bars for our pressure and temperature measurements on $\text{Fe}_{0.85}\text{Si}_{0.15}$ are shown in the bottom right corner. Open circles, *hcp*- $\text{Fe}_{0.85}\text{Si}_{0.15}$ only; solid triangles, coexistence of *hcp* and *bcc* phases; dashed lines, phase boundary between *hcp*- $\text{Fe}_{0.85}\text{Si}_{0.15}$ and *hcp/bcc* Fe-Si alloys from this study, Lin *et al.* [2002a], and Lin [2002]; grey hexagon, *bcc*- $\text{Fe}_{0.9}\text{Ni}_{0.1}$ at 225 GPa and 3400 K [Dubrovinsky *et al.*, 2007]; dash-dotted and dotted lines, theoretically predicted melting curve of Fe by Alfe *et al.* [2002] and Laio *et al.* [2000], respectively; open triangle, square, and diamond, melting data on pure Fe from shock-wave experiments by Ahrens *et al.* [2002], Brown and McQueen [1986], and Nguyen and Holmes [2004], respectively.

¹Auxiliary materials are available in the HTML. doi:10.1029/2008GL036990.

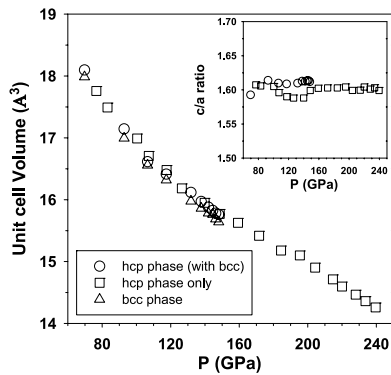


Figure 3. Unit cell parameters of the Si-rich *bcc* (red open triangles) and Si-poor *hcp* phases (blue open circles) at high pressures and room temperature. Lattice parameters of the *hcp*-Fe_{0.85}Si_{0.15} phase alone (without coexistence with the *bcc* phase; black open squares) are also plotted for comparison. The coexisting *bcc* and *hcp* phases were produced at 148 GPa and high temperatures (Figure 2) and decompressed at room temperature. Insert, axial ratio (*c/a*) of the *hcp* phase.

lower-pressure results (Figure 1). These results show that the volume ratio of the *bcc* phase to the *hcp* phase increases with increasing temperature and decreases with increasing pressure (Figure 1) (see also Lin [2002] for detail of the diffraction patterns in the *bcc* + *hcp* coexistence region), indicating that the *hcp* phase is the stable phase at higher pressures.

[7] Since most intense diffraction peaks of the suspected *hcp*, *bcc*, *fcc*, and *b2* phases of Fe-Si alloys are very close to each other according to previous reports [Lin *et al.*, 2002a; Dubrovinsky *et al.*, 2003; Asanuma *et al.*, 2008] (Figure 2), we moved the CCD to various distances from the sample to increase the spatial resolution of the diffraction peaks for phase identification in particular regions of interest. We observed no X-ray diffraction evidence of the previously reported *fcc* or *b2* phases of the Fe-Si alloy. The molar volume of the *bcc* phase is about 1% smaller than that of the coexisting *hcp* at 143 GPa and 300 K, whereas its incompressibility based on experimental data between 60 GPa and 143 GPa is similar to those of the *hcp*-Fe_{0.85}Si_{0.15} [Lin *et al.*, 2003a] and *hcp*-Fe phases [Mao *et al.*, 1990] (Figure 3). Our measured *c/a* axial ratio of the *hcp*-Fe_{0.85}Si_{0.15} phase remains almost constant at 1.60 (± 0.01) up to 240 GPa. Using unit cell parameters determined from this study and the compositional difference of 4 atomic % in Si between the lower-density Si-rich *bcc* and higher-density Si-poor *hcp* phases reported by Lin *et al.* [2002a; Lin, 2002], the density difference between the *bcc* and *hcp* phases is approximately 2% at 100–150 GPa.

4. Discussion and Geophysical Applications

[8] Compared to the phase diagram of pure Fe (Figure 2), it is evident that *hcp*-Fe_{0.85}Si_{0.15} is stable as a single phase between 170 GPa and 240 GPa at high temperatures, whereas it separates into a mixture of the *bcc* and *hcp* Fe-Si phases at lower pressures up to at least 150 GPa at high temperatures. To explain X-ray diffraction patterns of Fe-Si alloys, here we further discuss the stacking sequences of the Fe polymorphs. The layered dense-packed structure of Fe and Fe-rich alloys

can result in various stacking polymorphs—*hcp* phase with *ABAB* stacking sequence along [001], *fcc* with *ABCABC* stacking along [111], and doubled *hcp* phase with *ABAC* stacking along [001]. Because of the similarities in the stacking layers, the difference in the Gibbs free energy between these phases at high pressures and temperatures is very small, and variations in experimental conditions such as temperature gradient have been shown to result in the occurrence of the *fcc* or doubled *hcp* phase at high pressures and temperatures. The *hcp* and *fcc* phases share the same lattice plane in the stacking layers along [001] and [111], respectively, which are manifested in their overlapping diffraction peaks in *hcp* (002) and *fcc* (111) in Fe and Fe-Si alloys over a wide pressure-temperature range (Figure 1b) [e.g., Shen *et al.*, 1998; Lin *et al.*, 2002a; Lin, 2002; Mikhaylushkin *et al.*, 2007]. The large splitting between the assigned *hcp* (002) and *fcc* (111) peaks for Fe_{0.93}Si_{0.07} by Asanuma *et al.* [2008], however, contradicts the aforementioned statement and cannot be explained by the occurrence of the metastable *fcc* phase alone, indicating that this assignment is most likely incorrect.

[9] Dubrovinsky *et al.* [2003] reported that Fe-rich Fe-Si alloys dissociate into almost pure *hcp*-Fe and *b2*-structured FeSi with the 1:1 atomic ratio at high pressures and temperatures, indicating the occurrence of an immiscibility gap between the phases. Their transition boundary between the *hcp* and *hcp* + *b2* regions had a negative slope, and the transition from the low-pressure *bcc* Fe-Si alloy to the high-pressure *b2*-structured FeSi phase is discontinuous [Dubrovinsky *et al.*, 2003], inconsistent with our results and previous experimental and theoretical studies [Lin *et al.*, 2002a; Cote *et al.*, 2008a, 2008b]. The *b2*-structured FeSi with the 1:1 atomic ratio reported by Dubrovinsky *et al.* [2003] is the fully ordered form of the *bcc* Fe-Si alloy, requiring a significant amount of Si partitioned into the phase. We note that beside different origins of the samples Dubrovinsky *et al.* [2003] mainly used electrically-heated DAC experiments with hours of heating before the observation of the *b2*-structured FeSi phase, while their laser-heated DAC experiments were conducted offline. It is thus conceivable that a small amount of carbon diffusion from the diamond anvils to the sample in the long time heating experiments [Prakapenka *et al.*, 2003] could stabilize this phase, which in turn may affect the slope of the phase boundary. In our on-line high pressure-temperature experiments we have detected *in-situ* effect of temperature cycling on appearance-disappearance of the *bcc* phase that is necessary to constrain phase boundary slope. Based on our current and previous studies [Lin *et al.*, 2002a], we observed the *bcc* phase coexisted with the *hcp* phase but found no evidence for the *b2* (100) reflection. We note that the compositional difference in Si between the *bcc* and *hcp* phases is approximately 3–4 atomic % [Lin *et al.*, 2002a], which is clearly insufficient to form the fully ordered *b2*-structured FeSi phase.

[10] Previous studies estimate that an inner core containing about 4 wt% Si in Fe would satisfy seismological constraints. Our results on Fe_{0.85}Si_{0.15} alloy (with 8 wt% Si) up to 240 GPa and 3000 K show that it is stable in the *hcp* phase above 170 GPa at high temperatures (Figure 3), suggesting Fe-Si alloy is likely in the *hcp* structure in the inner core, instead of a previously proposed mixture of *hcp* and *bcc*

phases [Lin *et al.*, 2002a]. However, the additional effect of Ni in stabilizing the *fcc* or *bcc* phases and the predicted occurrence of *bcc*-Fe in the core all remain to be further investigated [e.g., Lin *et al.*, 2002b; Voadlo *et al.*, 2003; Mao *et al.*, 2006; Dubrovinsky *et al.*, 2007; Belonoshko *et al.*, 2008; Kuwayama *et al.*, 2008].

[11] The observed mixture of the *bcc* and *hcp* alloys up to at least 150 GPa and 3000 K may have implications for our understanding of the properties of the outer core (Figure 2). The Si-rich *bcc* and Si-poor *hcp* phases should have different melting points at their coexisting pressures due to their compositional and structural differences, which could provide a mechanism for Si partitioning between liquid and solid Fe in the core. Based on the concept that the local structure and properties of a liquid mimics that of a relevant solid [Sanloup *et al.*, 2000; Shen *et al.*, 2004], the volumetric dominance of the *hcp* phase in the *hcp* + *bcc* coexistence region indicates that the dense closest-packed Fe-Si liquid is more relevant to understanding the properties of the liquid outer core.

[12] **Acknowledgments.** We acknowledge GSECARS, APS, and ANL for the use of the synchrotron and laser facilities. Use of the Advanced Photon Source is supported by U.S. Department of Energy, Office of Science, Basic Energy Sciences, under contract DE-AC02-06CH11357. GSECARS is supported by NSF Earth Sciences (EAR-0622171) and DOE Geosciences (DE-FG02-94ER14466). R. A. F. and Y.-Y. C. are supported by grants from the NSF (EAR-0748707) and the Carnegie/DOE Alliance Center (CDAC) to S. D. Jacobsen. We thank S. Grand for his fruitful discussions. J. F. L. acknowledges financial support from NSF Earth Sciences (EAR-0838221) and CDAC.

References

- Ahrens, T. J., K. G. Holland, and C. Q. Chen (2002), Phase diagram of iron, revised-core temperatures, *Geophys. Res. Lett.*, *29*(7), 1150, doi:10.1029/2001GL014350.
- Alfe, D., G. D. Price, and M. J. Gillan (2002), Iron under Earth's core conditions: Liquid-state thermodynamics and high-pressure melting curve from *ab initio* calculations, *Phys. Rev. B*, *65*, 165118, doi:10.1103/PhysRevB.65.165118.
- Asanuma, H., E. Ohtani, T. Sakai, H. Terasaki, S. Kamada, N. Hirao, N. Sata, and Y. Ohishi (2008), Phase relations of Fe-Si alloy up to core conditions: Implications for the Earth inner core, *Geophys. Res. Lett.*, *35*, L12307, doi:10.1029/2008GL033863.
- Belonoshko, A. B., *et al.* (2008), Elastic anisotropy of Earth's inner core, *Science*, *319*, 797–800.
- Birch, F. (1952), Elasticity and constitution of the Earth's interior, *J. Geophys. Res.*, *57*, 227–286.
- Brown, J. M., and R. G. McQueen (1986), Phase transitions, Grüneisen parameter, and elasticity for shocked iron between 77 GPa and 400 GPa, *J. Geophys. Res.*, *91*, 7485–7494.
- Cote, A. S., L. Voadlo, and J. P. Brodholt (2008a), Light elements in the core: Effects of impurities on the phase diagram of iron, *Geophys. Res. Lett.*, *35*, L05306, doi:10.1029/2007GL032788.
- Cote, A. S., L. Voadlo, and J. P. Brodholt (2008b), The effect of silicon impurities on the phase diagram of iron and possible implications for the Earth's core structure, *J. Phys. Chem. Solids*, *69*, 2177–2181.
- Dubrovinsky, L. S., *et al.* (2003), Iron-silica interaction at extreme conditions and the electrically conducting layer at the base of Earth's mantle, *Nature*, *422*, 58–61.
- Dubrovinsky, L., *et al.* (2007), Body-centered cubic iron-nickel alloy in Earth's core, *Science*, *316*, 1880–1883.
- Fei, Y., *et al.* (2007), Toward an internally consistent pressure scale, *Proc. Natl. Acad. Sci. U. S. A.*, *104*, 9182–9186.
- Hirao, N., E. Ohtani, T. Kondo, and T. Kikegawa (2004), Equation of state of iron-silicon alloys to megabar pressure, *Phys. Chem. Miner.*, *31*, 329–336.
- Kuwayama, Y., K. Hirose, N. Sata, and Y. Ohishi (2008), Phase relations of iron and iron-nickel alloys up to 300 GPa: Implications for composition and structure of the Earth's inner core, *Earth Planet. Sci. Lett.*, *273*, 379–385.
- Laio, A., S. Bernard, G. L. Chiarotti, S. Scandolo, and E. Tosatti (2000), Physics of iron at Earth's core conditions, *Science*, *287*, 1027–1030.
- Li, J., and Y. Fei (2003), Experimental constraints on core composition, *Treatise Geochem.*, *2*, 521–546.
- Lin, J.-F. (2002), Alloying effects of silicon and nickel on iron in the Earth's core, Ph.D. thesis, 126 pp., Univ. of Chicago, Chicago, Ill.
- Lin, J., D. L. Heinz, A. J. Campbell, J. M. Devine, and G. Shen (2002a), Iron-silicon alloy in Earth's core?, *Science*, *295*, 313–315.
- Lin, J.-F., *et al.* (2002b), Iron-nickel alloy in the Earth's core, *Geophys. Res. Lett.*, *29*(10), 1471, doi:10.1029/2002GL015089.
- Lin, J.-F., A. J. Campbell, D. L. Heinz, and G. Shen (2003a), Static compression of iron-silicon alloys: Implications for silicon in the Earth's core, *J. Geophys. Res.*, *108*(B1), 2045, doi:10.1029/2002JB001978.
- Lin, J.-F., V. V. Struzhkin, W. Sturhahn, E. Huang, J. Zhao, M. Y. Hu, E. E. Alp, H. Mao, N. Boctor, and R. J. Hemley (2003b), Sound velocities of iron-nickel and iron-silicon alloys at high pressures, *Geophys. Res. Lett.*, *30*(21), 2112, doi:10.1029/2003GL018405.
- Ma, Y., *et al.* (2004), In situ X-ray diffraction studies of iron to Earth-core conditions, *Phys. Earth Planet. Inter.*, *143*, 455–467.
- Mao, H. K., Y. Wu, L. C. Chen, J. F. Shu, and A. P. Jephcoat (1990), Static compression of iron to 300 GPa and Fe_{0.8}Ni_{0.2} alloy to 260 GPa: Implications for composition of the core, *J. Geophys. Res.*, *95*, 21,737–21,742.
- Mao, W. L., A. J. Campbell, D. L. Heinz, and G. Shen (2006), Phase relations of Fe-Ni alloys at high pressure and temperature, *Phys. Earth Planet. Inter.*, *155*, 146–151.
- Mikhailushkin, A. S., *et al.* (2007), Pure iron compressed and heated to extreme conditions, *Phys. Rev. Lett.*, *99*, 165505, doi:10.1103/PhysRevLett.99.165505.
- Nguyen, J. H., and N. C. Holmes (2004), Melting of iron at the physical conditions of the Earth's core, *Nature*, *427*, 339–342.
- Poirier, J. P. (1994), Light elements in the Earth's outer core: A critical review, *Phys. Earth Planet. Inter.*, *85*, 319–337.
- Prakapenka, V. B., *et al.* (2003), Carbon transport in diamond anvil cells, *High Temp. High Pressures*, *35/36*, 237–249.
- Prakapenka, V. B., *et al.* (2008), Advanced flat top laser heating system for high pressure research at GSECARS: Application to the melting behavior of germanium, *High Pressure Res.*, *28*, 225–235.
- Sakai, T., T. Kondo, E. Ohtani, H. Terasaki, N. Endo, T. Kuba, T. Suzuki, and T. Kikegawa (2006), Interaction between iron and post-perovskite at core-mantle boundary and core signature in plume source region, *Geophys. Res. Lett.*, *33*, L15317, doi:10.1029/2006GL026868.
- Sanloup, C., *et al.* (2000), Structural changes in liquid Fe at high pressures and high temperatures from synchrotron X-ray diffraction, *Europhys. Lett.*, *52*, 151–157.
- Shen, G., H. K. Mao, R. J. Hemley, T. S. Duffy, and M. L. Rivers (1998), Melting and crystal structure of iron at high pressures and temperatures, *Geophys. Res. Lett.*, *25*, 276–373.
- Shen, G., V. B. Prakapenka, M. L. Rivers, and S. R. Sutton (2004), Structure of liquid iron at pressures up to 58 GPa, *Phys. Rev. Lett.*, *92*, 185701, doi:10.1103/PhysRevLett.92.185701.
- Takafuji, N., K. Hirose, M. Mitome, and Y. Bando (2005), Solubilities of O and Si in liquid iron in equilibrium with (Mg,Fe)SiO₃ perovskite and the light elements in the core, *Geophys. Res. Lett.*, *32*, L06313, doi:10.1029/2005GL022773.
- Voadlo, L., *et al.* (2003), Possible thermal and chemical stabilization of body-centred-cubic iron in the Earth's core, *Nature*, *424*, 536–539.

Y.-Y. Chang and R. A. Fischer, Department of Earth and Planetary Sciences, Northwestern University, Evanston, IL 60208, USA.

I. Kantor and V. B. Prakapenka, Consortium for Advanced Radiation Sources, University of Chicago, Chicago, IL 60637, USA.

J.-F. Lin, Department of Geological Sciences, Jackson School of Geosciences, University of Texas at Austin, Austin, TX 78712, USA. (afu@jsg.utexas.edu)

H. P. Scott, Department of Physics and Astronomy, Indiana University, South Bend, IN 46634, USA.